2360 *Inorg. Chem.* **2010**, *49*, 2360–2371
DOI: 10.1021/ic902271x

Inorganic Chemistry
Article

Ring-Opening Polymerization of Lactides Catalyzed by Natural Amino-Acid Based Zinc Catalysts

Donald J. Darensbourg* and Osit Karroonnirun

Department of Chemistry, Texas A&M University, College Station, Texas 77843

Received November 16, 2009

A series of chiral NNO-tridentate Schiff base ligands derived from natural amino acids were reacted with zinc(*bis*-trimethylsilylamide)$_2$ to provide metal complexes which have been fully characterized. One of these derivatives was further reacted with *p*-fluorophenol to yield a phenoxide complex. X-ray crystallographic studies reveal the zinc Schiff base amide complexes to be monomeric, whereas, the *p*-fluorophenolate complex was shown to be dimeric with bridging phenoxide ligands. All zinc complexes were shown to be very effective catalysts for the ring-opening polymerization (ROP) of lactides at ambient temperature, producing polymers with controlled and narrow molecular weight distributions. These enantiomerically pure zinc complexes did not show selectivity toward either L- or D-lactide, that is, $k_{D(obsd)}/k_{L(obsd)} \approx 1$. However, steric substituents on the Schiff base ligands exhibited moderate to excellent stereocontrol for the ROP of *rac*-lactide. Heterotactic polylactides were produced from *rac*-lactide with P_r values ranging from 0.68 to 0.89, depending on the catalyst employed and the reaction temperature. The reactivities of the various catalysts were greatly affected by substituents on the Schiff base ligands, with sterically bulky substituents being rate enhancing.

Introduction

Presently there is considerable interest in synthesizing useful polymeric materials wholly or in part from renewable resources.[1] For example, major efforts are underway for industrially preparing the most widely used polymers worldwide, polyethylene and poly(ethylene terephthalate), from renewable resources, that is, ethanol-based ethylene[2] and ethylene glycol derived from sugar and molasses.[3] Polyesters represent another class of polymers that can serve as alternative materials for petrochemical-based polymers and are derived from 100% renewable resources. That is, polylactides are aliphatic polyesters obtained by polymerizing lactic acid which is available from the fermentation of sugar (beet or cane) or starch (corn, wheat, potatoes, or manioc). Of importance, these polymers have the highly desirable properties of biocompatibility and biodegradability. As a consequence, polymers such as polylactides have been widely used in medical applications, such as, biodegradable sutures, slow release drug delivery, and tissue engineering.[4−6]

The use of metal-based catalysts for the ring-opening polymerization (ROP) of cyclic esters has been the subject of several reviews.[4,7−9] Included in these studies are metal complexes

*To whom correspondence should be addressed. E-mail: djdarens@mail.chem.tamu.edu. Fax (979)845-0158.

(1) (a) Williams, C. K.; Hillmyer, M. A. *Polym. Rev.* **2008**, *48*, 1–10. (b) Gandini, A. *Macromolecules* **2008**, *41*, 9491–9504. (c) Coates, G. W.; Hillmyer, M. A. *Macromolecules* **2009**, *42*, 7987–7989.
(2) Morschbacker, A. *Polym. Rev.* **2009**, *49*, 79–84.
(3) (a) *C&E News* **2009**, *87*, No. 21, 9. (b) *Sci. News. Phys. Chem.* **2008**, September 23.
(4) Platel, R. H.; Hodgson, L. M.; Williams, C. K. *Polym. Rev.* **2008**, *48*, 11–63.
(5) Ikada, Y.; Tsuji, H. *Macromol. Rapid Commun.* **2000**, *21*, 117–132.
(6) Penco, M.; Donetti, R.; Mendichi, R.; Ferruti, P. *Macromol. Chem. Phys.* **1998**, *199*, 1737–1745.
(7) O'Keefe, B. J.; Hillmyer, M. A.; Tolman, W. B. *J. Chem. Soc., Dalton Trans.* **2001**, 2215–2224.
(8) Dechy-Cabaret, O.; Martin-Vaca, B.; Bourissou, D. *Chem. Rev.* **2004**, *104*, 6147–6176.
(9) Kamber, N. E.; Jeong, W.; Waymouth, R. M.; Pratt, R. C.; Lohmeijer, B. G. G.; Hedrick, J. L. *Chem. Rev.* **2007**, *107*, 5813–5840.
(10) Pospiech, D.; Komber, H.; Jehnichen, D.; Haussler, L.; Eckstein, K.; Scheibner, H.; Janke, A.; Kricheldorf, H. R.; Petermann, O. *Biomacromolecules* **2005**, *6*, 439–446.
(11) Ruckenstein, E.; Yuan, Y. *J. Appl. Polym. Sci.* **1998**, *69*, 1429–1434.
(12) Kricheldorf, H. R.; Stricker, A. *Macromol. Chem. Phys.* **1999**, *200*, 1726–1733.
(13) Chisholm, M. H.; Gallucci, J. C.; Krempner, C. *Polyhedron* **2007**, *26*, 4436–4444.
(14) Grafov, A.; Vuorinen, S.; Repo, T.; Kemell, M.; Nieger, M.; Leskelä, M. *Eur. Polym. J.* **2008**, *44*, 3797–3805.
(15) Chmura, A. J.; Chuck, C. J.; Davidson, M. G.; Jones, M. D.; Lunn, M. D.; Bull, S. D.; Mahon, M. F. *Angew. Chem., Int. Ed.* **2007**, *46*, 2280–2283.
(16) Simic, V.; Pensec, S.; Spassky, N. *Macromol. Symp.* **2000**, *153*, 109–121.
(17) O'Keefe, B. J.; Breyfogle, L. E.; Hillmyer, M. A.; Tolman, W. B. *J. Am. Chem. Soc.* **2002**, *124*, 4384–4393.
(18) Wang, X.; Liao, K.; Quan, D.; Wu, Q. *Macromolecules* **2005**, *38*, 4611–4617.
(19) Stolt, M.; Krasowska, K.; Rutkowska, M.; Janik, H.; Rosling, A.; Södergård, A. *Polym. Int.* **2005**, *54*, 362–368.
(20) McGuinness, D. S.; Marshall, E. L.; Gibson, V. C.; Steed, J. W. *J. Polym. Sci., Part A: Polym. Chem.* **2003**, *41*, 3798–3803.

Published on Web 02/01/2010

of Sn,[10−14] Ge,[15] Y,[16] Fe,[17−23] Ti/Zr,[14,24−33] Mg,[34−48] Al,[49−73] Ca,[35,74−77] Na,[78] Li,[79] Zn,[34−36,43,44,47,48,55,80−101] and In.[102−104] Although a large variety of metal derivatives effectively catalyzes the ROP of lactide, it is preferable to use biocompatible metals since polylactides are widely utilized in food packaging and biomedical applications. Because the lactide monomer consists of two stereocenters, it exists as three possible stereoisomers, L-lactide, D-lactide, and *meso*-lactide. The extent of stereocontrol exhibited by a catalytic system is very important because the physical and degradation properties of the polylactide depend upon the tacticity of the polymer. Isotactic L- or D-polylactides can easily be obtained from enantiomerically pure L- or D-lactide, respectively. However, upon polymerizing *rac*- or *meso*-lactide, selective catalysts greatly influence the tacticity of the resulting polymeric material. For example, utilizing a catalyst system with stereocontrol syndiotactic polylactide and heterotactic polylactide can be synthesized from *meso*- or *rac*-lactide, respectively. These processes are depicted in eqs 1 and 2.

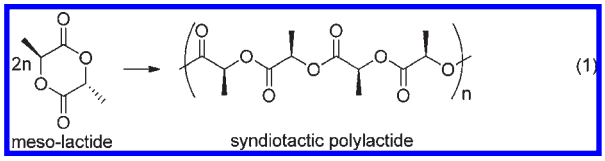

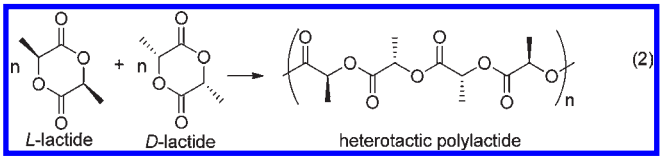

In addition, stereocomplexed polylactides can be produced from a blend of poly-L-lactide acid (PLLA) and poly-D-lactide acid (PDLA) which have a T_m value of 230 °C,[105−107] while homocrystallized polylactides have melting temperatures in the range of 170−180 °C.[108] An increase in T_m coupled with different physical and mechanical properties relative to the parent homopolymers makes the stereocomplexed polylactide an attractive polymer (eq 3). Because the properties of polylactide are so highly dependent on the polymer's tacticity,[8,109,110] research studies employing chiral catalysts for the ROP of lactides where enantiomorphic site control is possible are of much current interest.

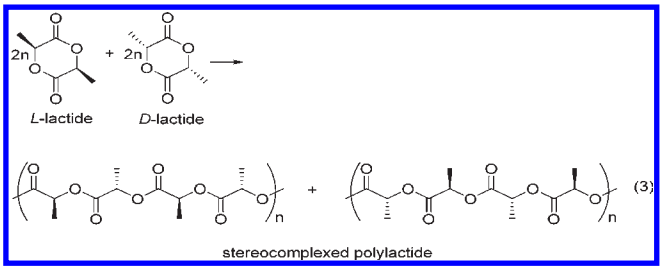

Herein we wish to describe the synthesis of chiral Schiff base ligands derived from the natural amino acids, L-phenylalanine,

(21) Gibson, V. C.; Marshall, E. L.; Navarro-Llobet, D.; White, A. J. P.; Williams, D. J. *J. Chem. Soc., Dalton Trans.* **2002**, 4321–4322.
(22) O'Keefe, B. J.; Monnier, S. M.; Hillmyer, M. A.; Tolman, W. B. *J. Am. Chem. Soc.* **2001**, *123*, 339–340.
(23) Stolt, M.; Södergård, A. *Macromolecules* **1999**, *32*, 6412–6417.
(24) Russell, S. K.; Gamble, C. L.; Gibbins, K. J.; Juhl, K. C. S.; Mitchell, W. S.; Tumas, A. J.; Hofmeister, G. E. *Macromolecules* **2005**, *38*, 10336–10340.
(25) Chmura, A. J.; Davidson, M. G.; Jones, M. D.; Lunn, M. D.; Mahon, M. F.; Johnson, A. F.; Khunkamchoo, P.; Roberts, S. L.; Wong, S. S. F. *Macromolecules* **2006**, *39*, 7250–7257.
(26) Gregson, C. K. A.; Gibson, V. C.; Long, N. J.; Marshall, E. L.; Oxford, P. J.; White, A. J. P. *J. Am. Chem. Soc.* **2006**, *128*, 7410–7411.
(27) Gendler, S.; Segal, S.; Goldberg, I.; Goldschmidt, Z.; Kol, M. *Inorg. Chem.* **2006**, *45*, 4783–4790.
(28) Chmura, A. J.; Davidson, M. G.; Jones, M. D.; Lunn, M. D.; Mahon, M. F. *Dalton Trans.* **2006**, 887–889.
(29) Atkinson, R. C. J.; Gerry, K.; Gibson, V. C.; Long, N. J.; Marshall, E. L.; West, L. J. *Organometallics* **2006**, *26*, 316–320.
(30) Kim, Y.; Verkade, J. G. *Organometallics* **2002**, *21*, 2395–2399.
(31) Kim, Y.; Jnaneshwara, G. K.; Verkade, J. G. *Inorg. Chem.* **2003**, *42*, 1437–1447.
(32) Lee, J.; Kim, Y.; Do, Y. *Inorg. Chem.* **2007**, *46*, 7701–7703.
(33) Chmura, A. J.; Cousins, D. M.; Davidson, M. G.; Jones, M. D.; Lunn, M. D.; Mahon, M. F. *Dalton Trans.* **2008**, 1437–1443.
(34) Tsai, Y.-H.; Lin, C.-H.; Lin, C.-C.; Ko, B.-T. *J. Polym. Sci., Part A: Polym. Chem.* **2009**, *47*, 4927–4936.
(35) Wheaton, C. A.; Hayes, P. G.; Ireland, B. J. *Dalton Trans.* **2009**, 4832–4846.
(36) Huang, Y.; Hung, W.-C.; Liao, M.-Y.; Tsai, T.-E.; Peng, Y.-L.; Lin, C.-C. *J. Polym. Sci., Part A: Polym. Chem.* **2009**, *47*, 2318–2329.
(37) Hung, W.-C.; Lin, C.-C. *Inorg. Chem.* **2009**, *48*, 728–734.
(38) Wu, J.; Chen, Y.-Z.; Hung, W.-C.; Lin, C.-C. *Organometallics* **2008**, *27*, 4970–4978.
(39) Tang, H.-Y.; Chen, H.-Y.; Huang, J.-H.; Lin, C.-C. *Macromolecules* **2007**, *40*, 8855–8860.
(40) Sánchez-Barba, L. F.; Garcés, A.; Fajardo, M.; Alonso-Moreno, C.; Fernández-Baeza, J.; Otero, A.; Antiñolo, A.; Tejeda, J.; Lara-Sánchez, A.; López-Solera, M. I. *Organometallics* **2007**, *26*, 6403–6411.
(41) Lian, B.; Thomas, C. M.; Casagrande, O. L., Jr.; Roisnel, T.; Carpentier, J.-F. *Polyhedron* **2007**, *26*, 3817–3824.
(42) Sánchez-Barba, L. F.; Hughes, D. L.; Humphrey, S. M.; Bochmann, M. *Organometallics* **2006**, *25*, 1012–1020.
(43) Wu, J.-C.; Huang, B.-H.; Hsueh, M.-L.; Lai, S.-L.; Lin, C.-C. *Polymer* **2005**, *46*, 9784–9792.
(44) Chisholm, M. H.; Gallucci, J. C.; Phomphrai, K. *Inorg. Chem.* **2005**, *44*, 8004–8010.
(45) Yu, T.-L.; Wu, C.-C.; Chen, C.-C.; Huang, B.-H.; Wu, J.; Lin, C.-C. *Polymer* **2005**, *46*, 5909–5917.
(46) Ejfler, J.; Michal, K.; Jerzykiewicz, L. B.; Sobota, P. *Dalton Trans.* **2005**, 2047–2050.
(47) Dove, A. P.; Gibson, V. C.; Marshall, E. L.; White, A. J. P.; Williams, D. J. *Dalton Trans.* **2004**, 570–578.
(48) Chisholm, M. H.; Phomphrai, K. *Inorg. Chim. Acta* **2003**, *350*, 121–125.
(49) Du, H.; Velders, A. H.; Dijkstra, P. J.; Sun, J.; Zhong, Z.; Chen, X.; Feijen, J. *Chem.—Eur. J.* **2009**, *15*, 9836–9845.
(50) Pappalardo, D.; Annunziata, L.; Pellecchia, C. *Macromolecules* **2009**, *42*, 6056–6062.
(51) Alaaeddine, A.; Thomas, C. M.; Roisnel, T.; Carpentier, J.-F. *Organometallics* **2009**, *28*, 1469–1475.
(52) Du, H.; Velders, A. H.; Dijkstra, P. J.; Zhong, Z.; Chen, X.; Feijen, J. *Macromolecules* **2009**, *42*, 1058–1066.
(53) Bouyahyi, M.; Grunova, E.; Marquet, N.; Kirillov, E.; Thomas, C. M.; Roisnel, T.; Carpentier, J.-F. *Organometallics* **2008**, *27*, 5815–5825.
(54) Iwasa, N.; Fujiki, M.; Nomura, K. *J. Mol. Catal. A: Chem.* **2008**, *292*, 67–75.
(55) Zhang, C.; Wang, Z.-X. *J. Organomet. Chem.* **2008**, *693*, 3151–3158.
(56) Chisholm, M. H.; Gallucci, J. C.; Quisenberry, K. T.; Zhou, Z. *Inorg. Chem.* **2008**, *47*, 2613–2624.
(57) Wu, J.; Pan, X.; Tang, N.; Lin, C.-C. *Eur. Polym. J.* **2007**, *43*, 5040–5046.
(58) Nomura, N.; Ishii, R.; Yamamoto, Y.; Kondo, T. *Chem.—Eur. J.* **2007**, *13*, 4433–4451.
(59) Du, H.; Pang, X.; Yu, H.; Zhuang, X.; Chen, X.; Cui, D.; Wang, X.; Jing, X. *Macromolecules* **2007**, *40*, 1904–1913.
(60) Tang, Z.; Gibson, V. C. *Eur. Polym. J.* **2007**, *43*, 150–155.
(61) Tang, Z.; Pang, X.; Sun, J.; Du, H.; Chen, X.; Wang, X.; Jing, X. *J. Polym. Sci., Part A: Polym. Chem.* **2006**, *44*, 4932–4938.
(62) Tang, Z.; Yang, Y.; Pang, X.; Hu, J.; Chen, X.; Hu, N.; Jing, X. *J. App. Polym. Sci.* **2005**, *98*, 102–108.
(63) Ma, H.; Melillo, G.; Oliva, L.; Spaniol, T. P.; Englert, U.; Okuda, J. *Dalton Trans.* **2005**, 721–727.
(64) Doherty, S.; Errington, R. J.; Housley, N.; Clegg, W. *Organometallics* **2004**, *23*, 2382–2388.
(65) Tang, Z.; Chen, X.; Pang, X.; Yang, Y.; Zhang, X.; Jing, X. *Biomacromolecules* **2004**, *5*, 965–970.

L-leucine, and L-methionine and their complexes with the biocompatible metal, zinc. These metal derivatives have been fully characterized and all shown to be highly active catalysts for the ROP of lactides. Included in these studies is the selectivity of these chiral zinc catalysts for the ROP of L- and D-lactide, as well as the effect of the substituents on the Schiff base ligands on the tacticity of the polylactide afforded from *rac*-lactide.

Scheme 1

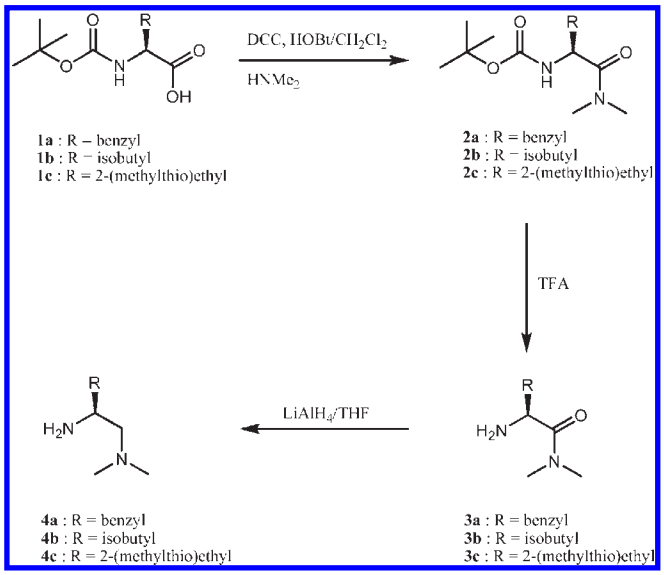

Results and Discussion

Synthesis and Characterization of Proligands and Their Zinc Complexes. The synthesis of chiral diamines **4a**−**c** is based on the reported literature[111] using different *N*-Boc-L-protected amino acids with modification as shown in Scheme 1. Condensation reactions of these diamines **4a**−**d** with 3,5-di-*tert*-butyl-2-hydroxybenzaldehyde at reflux in methanol yielded the analogous compounds **5a**−**d**, where R = benzyl, isobutyl, 2-(methylthio)ethyl, and hydrogen, respectively (Scheme 2). The reactions of these chiral ligands with zinc(*bis*-trimethylsilyl amide)$_2$, Zn[N(SiMe$_3$)$_2$]$_2$ in dry pentane resulted in straightforward formation of the yellow zinc complexes **6a**−**d**. In an analogous manner, the reaction of **5d** with Zn[N(SiMe$_3$)$_2$]$_2$ in the presence of *p*-fluorophenol yielded complex **6e** as shown in (Scheme 3). The complexes were characterized by ^{1}H and ^{13}C NMR spectroscopy, as well as, elemental analysis. The molecular structures of the complexes were determined by X-ray crystallography.

Suitable single crystals of complexes **6a**−**e** were obtained from recrystallization in dry pentane, and their molecular structures were determined by single X-ray crystallography. Complexes **6a**−**d** are very similar to each other. The solid-state structures of complexes **6a**−**d** have shown that two nitrogen atoms and one oxygen atom of the ligands coordinate to a metal center in a tridentate

(66) Li, H.; Wang, C.; Bai, F.; Yue, J.; Woo, H.-G. *Organometallics* **2004**, *23*, 1411–1415.
(67) Hormnirun, P.; Marshall, E. L.; Gibson, V. C.; White, A. J. P.; Williams, D. J. *J. Am. Chem. Soc.* **2004**, *126*, 2688–2689.
(68) Zhong, Z.; Dijkstra, P. J.; Feijen, J. *J. Am. Chem. Soc.* **2003**, *125*, 11291–11298.
(69) Zhong, Z.; Dijkstra, P. J.; Feijen, J. *Angew. Chem., Int. Ed.* **2002**, *41*, 4510–4513.
(70) Nomura, N.; Ishii, R.; Akakura, M.; Aoi, K. *J. Am. Chem. Soc.* **2002**, *124*, 5938–5939.
(71) Ovitt, T. M.; Coates, G. W. *J. Am. Chem. Soc.* **1999**, *121*, 4072–4073.
(72) Radano, C. P.; Baker, G. L.; Smith, M. R. *J. Am. Chem. Soc.* **2000**, *122*, 1552–1553.
(73) Cameron, P. A.; Jhurry, D.; Gibson, V. C.; White, A. J. P.; Williams, D. J.; Williams, S. *Macromol. Rapid Commun.* **1999**, *20*, 616–618.
(74) Zhong, Z.; Schneiderbauer, S.; Dijkstra, P. J.; Westerhausen, M.; Feijen, J. *Polym. Bull.* **2003**, *51*, 175–182.
(75) Darensbourg, D. J.; Choi, W.; Richers, C. P. *Macromolecules* **2007**, *40*, 3521–3523.
(76) Darensbourg, D. J.; Choi, W.; Karroonnirun, O.; Bhuvanesh, N. *Macromolecules* **2008**, *41*, 3493–3502.
(77) Chen, H.-Y.; Tang, H.-Y.; Lin, C.-C. *Polymer* **2007**, *48*, 2257–2262.
(78) Chen, H.-Y.; Zhang, J.; Lin, C.-C.; Reibenspies, J. H.; Miller, S. A. *Green Chem.* **2007**, *9*, 1038–1040.
(79) Hsueh, M.-L.; Huang, B.-H.; Wu, J.; Lin, C.-C. *Macromolecules* **2005**, *38*, 9482–9487.
(80) Börner, J.; Flörke, U.; Huber, K.; Döring, A.; Kuckling, D.; Herres-Pawlis, S. *Chem.—Eur. J.* **2009**, *15*, 2362–2376.
(81) Jones, M. D.; Davidson, M. G.; Keir, C. G.; Hughes, L. M.; Mahon, M. F.; Apperley, D. C. *Eur. J. Inorg. Chem.* **2009**, 635–642.
(82) Labourdette, G.; Lee, D. J.; Patrick, B. O.; Ezhova, M. B.; Mehrkhodavandi, P. *Organometallics* **2009**, *28*, 1309–1319.
(83) Hung, W.-C.; Huang, Y.; Lin, C.-C. *J. Polym. Sci., Part A: Polym. Chem.* **2008**, *46*, 6466–6476.
(84) Börner, J.; Herres-Pawlis, S.; Flörke, U.; Huber, K. *Eur. J. Inorg. Chem.* **2007**, 5645–5651.
(85) Bunge, S. D.; Lance, J. M.; Bertke, J. A. *Organometallics* **2007**, *26*, 6320–6328.
(86) Chen, C.-T.; Chen, C.-Y.; Huang, C.-A.; Chen, M.-T.; Peng, K.-F. *Dalton Trans.* **2007**, 4073–4078.
(87) Chen, H.-Y.; Tang, H.-Y.; Lin, C.-C. *Macromolecules* **2006**, *39*, 3745–3752.
(88) Jensen, T. R.; Schaller, C. P.; Hillmyer, M. A.; Tolman, W. B. *J. Organomet. Chem.* **2005**, *690*, 5881–5891.
(89) Bukhaltsev, E.; Frish, L.; Cohen, Y.; Vigalok, A. *Org. Lett.* **2005**, *7*, 5123–5126.
(90) Chen, H.-Y.; Huang, B.-H.; Lin, C.-C. *Macromolecules* **2005**, *38*, 5400–5405.
(91) Che, C.-M.; Huang, J.-S. *Coord. Chem. Rev.* **2003**, *242*, 97–113.
(92) Williams, C. K.; Breyfogle, L. E.; Choi, S. K.; Nam, W.; Young, V. G.; Hillmyer, M. A.; Tolman, W. B. *J. Am. Chem. Soc.* **2003**, *125*, 11350–11359.
(93) Hill, M. S.; Hitchcock, P. B. *J. Chem. Soc., Dalton Trans.* **2002**, 4694–4702.
(94) Williams, C. K.; Brooks, N. R.; Hillmyer, M. A.; Tolman, W. B. *Chem. Commun.* **2002**, 2132–2133.
(95) Chisholm, M. H.; Gallucci, J.; Phomphrai, K. *Inorg. Chem.* **2002**, *41*, 2785–2794.
(96) Chisholm, M. H.; Gallucci, J. C.; Zhen, H.; Huffman, J. C. *Inorg. Chem.* **2001**, *40*, 5051–5054.
(97) Chamberlain, B. M.; Cheng, M.; Moore, D. R.; Ovitt, T. M.; Lobkovsky, E. B.; Coates, G. W. *J. Am. Chem. Soc.* **2001**, *123*, 3229–3238.
(98) Chisholm, M. H.; Huffman, J. C.; Phomphrai, K. *J. Chem. Soc., Dalton Trans.* **2001**, 222–224.
(99) Cheng, M.; Attygalle, A. B.; Lobkovsky, E. B.; Coates, G. W. *J. Am. Chem. Soc.* **1999**, *121*, 11583–11584.
(100) Jensen, T. R.; Breyfogle, L. E.; Hillmyer, M. A.; Tolman, W. B. *Chem. Commun.* **2004**, 2504–2505.
(101) Labourdette, G.; Lee, D. J.; Patrick, B. O.; Ezhova, M. B.; Mehrkhodavandi, P. *Organometallics* **2009**, *28*, 1309–1319.
(102) Douglas, A. F.; Patrick, B. O.; Mehrkhodavandi, P. *Angew. Chem., Int. Ed.* **2008**, *47*, 2290–2293.
(103) Peckermann, I.; Kapelski, A.; Spaniol, T. P.; Okuda, J. *Inorg. Chem.* **2009**, *48*, 5526–5534.
(104) Pietrangelo, A.; Hillmyer, M. A.; Tolman, W. B. *Chem. Commun.* **2009**, 2736–2737.
(105) Kobayashi, K.; Sumitomo, H.; Itoigawa, T. *Macromolecules* **1987**, *20*, 906–908.
(106) Tsuji, H.; Ikada, Y. *Polymer* **1999**, *40*, 6699–6708.
(107) Sarasua, J.-R.; Prud'homme, R. E.; Wisniewski, M.; Le Borgne, A.; Spassky, N. *Macromolecules* **1998**, *31*, 3895–3905.
(108) Spinu, M.; Jackson, C.; Keating, M. Y. *J. Macromol. Sci., Pure, Appl. Chem.* **1996**, *A33*, 1497–1530.
(109) Chisholm, M. H.; Zhou, Z. *J. Mater. Chem.* **2004**, *14*, 3081–3092.
(110) Wu, J.; Yu, T.-L.; Chen, C.-T.; Lin, C.-C. *Coord. Chem. Rev.* **2006**, *250*, 602–626.
(111) Coldham, I.; O'Brien, P.; Patel, J. J.; Raimbault, S.; Sanderson, A. J.; Stead, D.; Whittaker, D. T. E. *Tetrahedron: Asym.* **2007**, *18*, 2113–2119.

Scheme 2

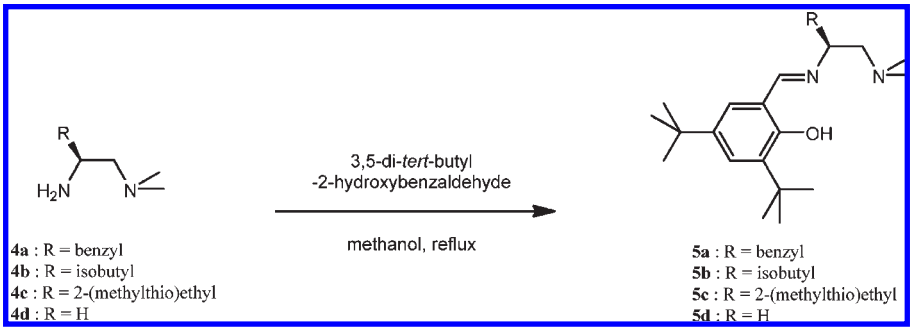

Scheme 3

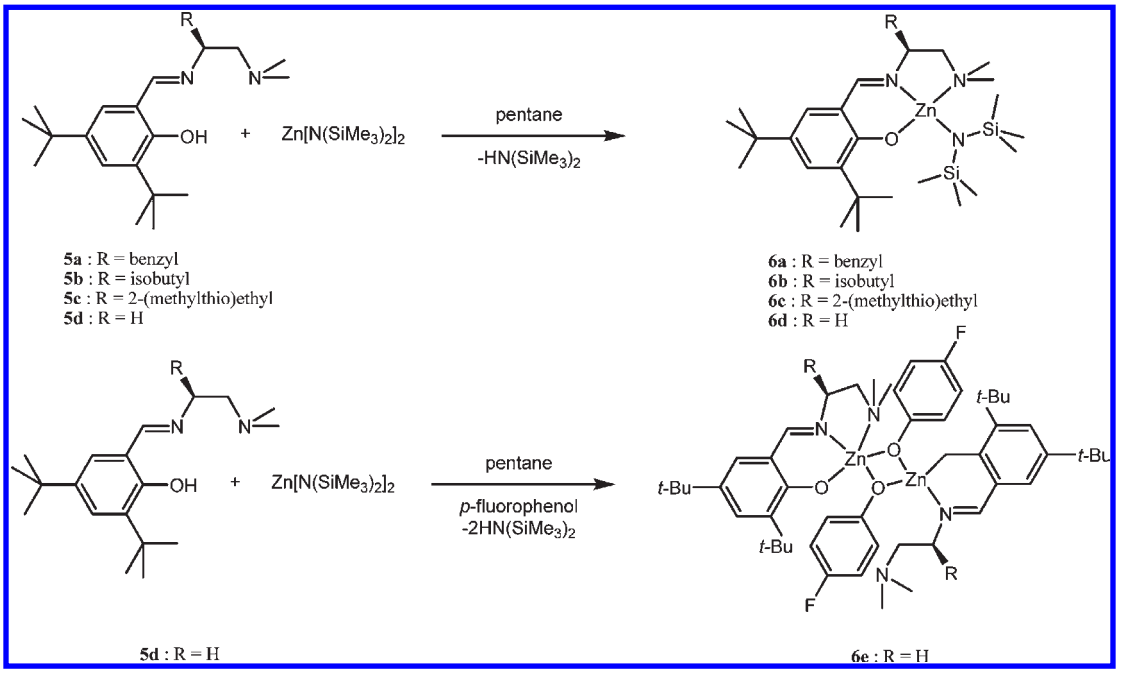

coordination mode along with one amido group. The geometry of the zinc complexes is a distorted tetrahedron with zinc at the center. The complexes are shown in Figure 1, with atomic labeling for non-hydrogen atoms. Selected bond distances and angles are listed in Table 1. On the other hand, if the amido group is replaced by *p*-fluorophenolate to give complex **6e**, the solid-state structure is shown to be dimeric with a Zn(1)/O(2)/Zn(2)/O(3) planar core bridged by the two oxygen atoms of *p*-fluorophenol as illustrated in Figure 2. The dimeric structure shows that one zinc center adopts a distorted tetrahedral geometry, in comparison with the other zinc center which possesses distorted trigonal bipyramidal geometry.

Polymerization Studies. Ring-Opening of Lactides. There are two different mechanisms for the stereoselective ROP of *rac*-lactide,[112] that is, a chain-end control[58] and an enantiomorphic site-control mechanism.[70,113] To examine this latter mechanism we have synthesized enantiomerically pure zinc complexes **6a**−**c**, and these plus the achiral complex **6d** were tested for the ROP of L- and D-lactide under the same reaction conditions to compare their selectivity and reactivity for this polymerization process. All reactions were carried out in C_6D_6 at ambient temperature and were monitored by ^{1}H NMR spectroscopy. The experimental observations reveal all zinc complexes to be active for the ROP of D- and L-lactide, and the resulting polymers were obtained with the expected molecular weights and with low polydispersity indices. To quantitatively compare the selectivity of each complex for the ROP of D- and L-lactide, the rates of the reactions were investigated. The polymerization reactions were found to be first-order in monomer as illustrated in Figure 3 for several catalytic systems. Table 2 summarizes the rate constants (k_{obsd}) for these various processes. As evident in Figure 3 and Table 2 the ratio of $k_{D(obsd)}$ over $k_{L(obsd)}$ is close to unity for reactions catalyzed by complexes **6a**−**c**, indicative of a lack of preferences of the enantiomerically pure complexes for L- or D-lactide. Complex **6a** was found to be the most active of the zinc complexes. The ROP of L-lactide utilizing the dimeric complex **6e** began slowly for the first 5 h, followed by a rate consistent with the more active monomeric catalyst **6d** (Figure 4). This is presumably due to dimeric disruption leading to a more active monomeric species as previously illustrated by Lin and co-workers.[87]

(112) Zhang, L.; Nederberg, F.; Messman, J. M.; Pratt, R. C.; Hedrick, J. L.; Wade, C. G. *J. Am. Chem. Soc.* **2007**, *129*, 12610–12611.
(113) Ovitt, T. M.; Coates, G. W. *J. Am. Chem. Soc.* **2002**, *124*, 1316–1326.

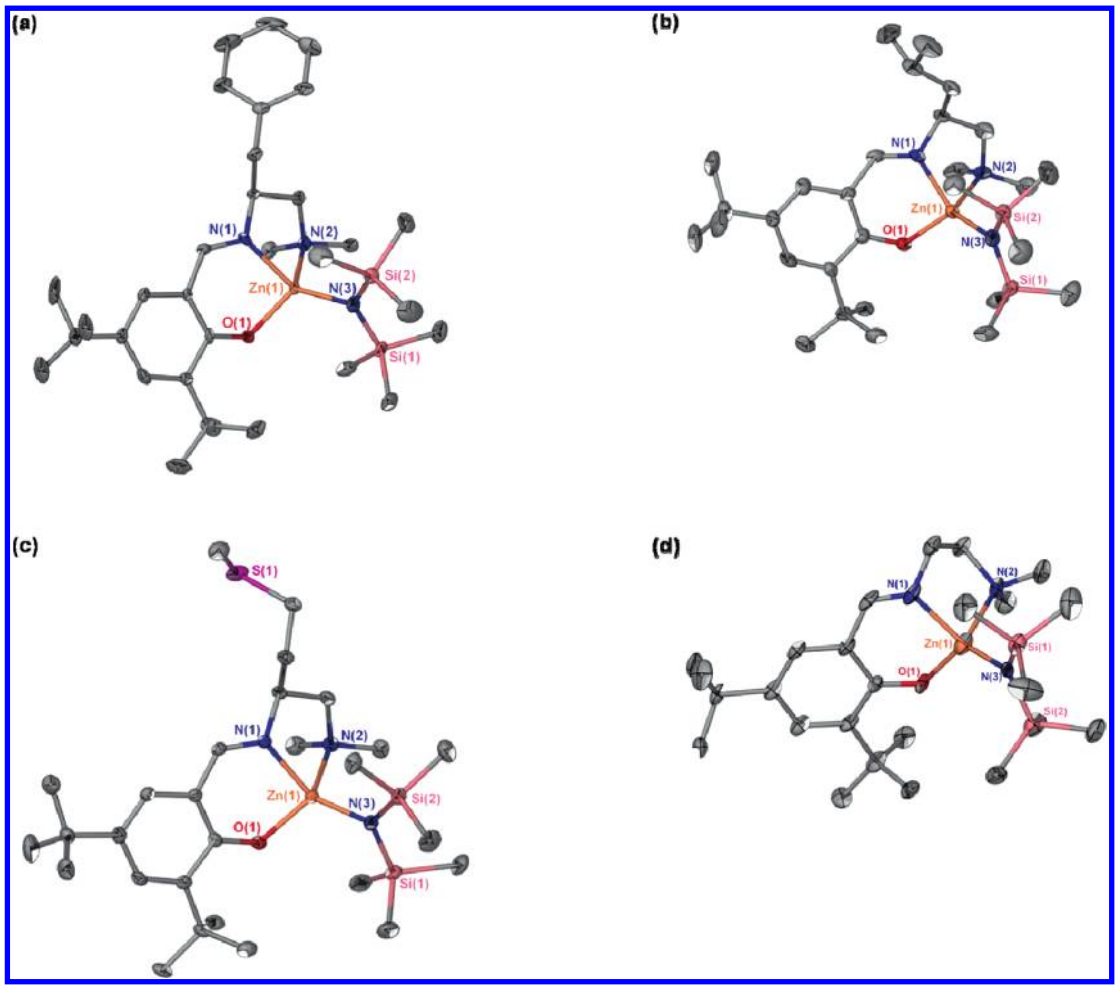

Figure 1. X-ray crystal structures of (a) **6a**, (b) **6b**, (c) **6c**, and (d) **6d**. Thermal ellipsoids represent the 50% probability surfaces. Hydrogen atoms are omitted for the sake of clarity.

Table 1. Selected Bond Lengths (Å) and Angles (deg) for Zn Complexes **6a**−**d**

	6a	**6b**	**6c**	**6d**
		Bond Lengths		
Zn1−N1	2.017 (4)	2.030 (4)	2.022 (2)	2.010 (5)
Zn1−N2	2.198 (3)	2.193 (4)	2.211 (2)	2.211 (6)
Zn1−N3	1.920 (4)	1.921 (4)	1.913 (2)	1.917 (5)
Zn1−O1	1.933 (3)	1.930 (3)	1.9406 (18)	1.930 (4)
		Bond Angles		
N3−Zn1−O1	115.60 (14)	119.64 (15)	116.01 (9)	122.2 (2)
N3−Zn1−N1	136.85 (16)	133.83 (15)	138.63 (9)	132.3 (2)
O1−Zn1−N1	91.24 (13)	92.20 (13)	91.58 (8)	90.6 (2)
N3−Zn1−N2	110.14 (14)	114.20 (16)	108.68 (9)	112.0 (2)
O1−Zn1−N2	121.26 (14)	112.07 (14)	120.65 (8)	110.9 (2)
N1−Zn1−N2	78.64 (14)	77.40 (14)	78.21 (8)	81.4 (2)

The rates of ROP of L-lactide in the presence of complex **6a** or **6d** were found to be independent of the addition of tetrahydrofuran (THF) to the benzene solvent. Figure 5 illustrate the lack of influence of significant concentrations of THF on k_{obsd} at ambient temperature for either of the catalyst systems. This is to be contrasted with comparable calcium complexes which were shown to be more active upon addition of the coordinating THF solvent.[76] That is, in this instance the larger calcium center is better able to expand its coordination number,

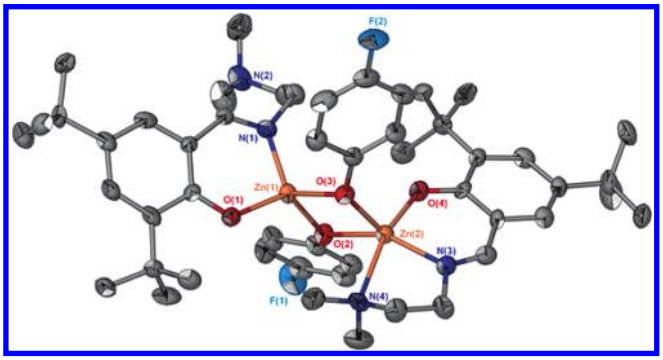

Figure 2. X-ray crystal structure of complex **6e**. Thermal ellipsoids represent the 50% probability surfaces. Hydrogen atoms are omitted for the sake of clarity. Selected bond lengths (Å) and angles (deg): Zn2−N3: 2.050 (6), Zn2−N4: 2.301 (5), Zn2−O2: 2.080 (4), Zn2−O3: 2.016 (5), Zn2−O4: 1.977 (4), O4−Zn2−O3: 106.69 (17), O4−Zn2−N3: 89.61 (18), O3−Zn2−N3: 126.78 (19), O4−Zn2−O2: 95.69 (16), O3−Zn2−O2: 80.79 (16), N3−Zn2−O2: 148.99 (18), O4−Zn2−N4: 161.08 (19), O3−Zn2−N4: 92.24 (18), N3−Zn2−N4: 78.79 (19), O2−Zn2−N4: 87.10 (17).

thereby enhancing the nucleophilicity of the propagating chain end.

As noted in Table 2 and Figure 3d, the rate of ROP of L-lactide for complex **6d** is slower than its more sterically hindered analogues, complexes **6a** and **6b**. Another

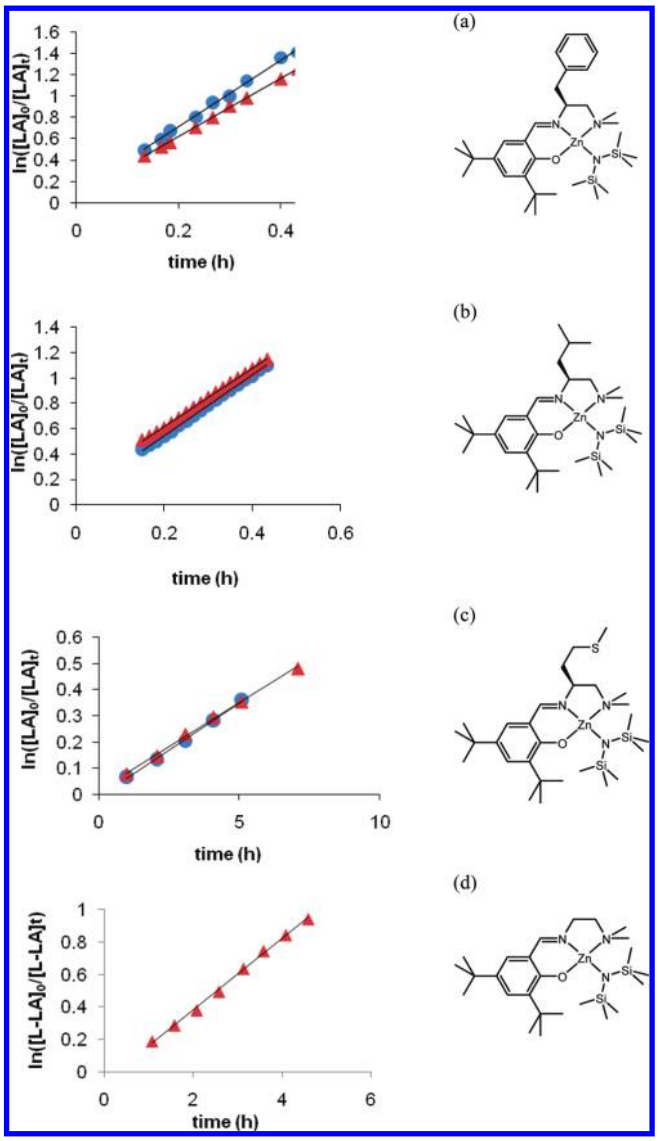

Figure 3. $\ln([LA]_0/[LA]_t)$ vs time plots for the ROP of D-lactide (blue solid circles) or L-lactide (red solid triangles) catalyzed by various zinc complexes at ambient temperature. (a) complex **6a**, (b) complex **6b**, (**c**) complex **6c**, and (d) complex **6d**.

differentiating feature noted for the ROP of L-lactide in the presence of complex **6d** is seen in the ^{1}H NMR spectra in C_6D_6 (Figure 6) during the catalytic reaction. That is, a methine proton resonance at 4.15 ppm is observed which corresponds to a *meso*-lactide, indicating that epimerization of the lactide monomer occurs during the polymerization process. This is further seen in the ROP of L-lactide catalyzed by complex **6d** where the anticipated isotactically pure polylactide exhibits small defects in microstructure as shown in Figure 7a. With the other closely related, but sterically more encumbered catalysts, complexes **6a**−**c**, this isomerization process is not observed as illustrated by the ^{1}H NMR spectrum of the polylactide in Figure 7b. In the case of complex **6c**, the sulfur atom from the amine backbone possibly coordinates to the zinc center following dissociation of the dimethylamine arm resulting in the slowest rate of catalysis for all the complexes (vide infra).

The ROP of *rac*-lactide catalyzed by complexes **6a**−**d** was performed in chloroform at ambient temperature.

Table 2. Rate Constants for the ROP of D- or L-Lactide in the Presence of Zinc Complexes[a]

entry	M	$k_{D(obsd)}$ (h^{-1})	$k_{L(obsd)}$ (h^{-1})	k_D/k_L
1	**6a**	3.13	2.73	1.14
2	**6b**	2.38	2.30	1.03
3	**6c**	0.07	0.06	1.16
4	**6d**		0.22	
5	**6e**		0.20[b]	

[a] Each reaction was performed in C_6D_6 at ambient temperature. Monomer and catalyst concentrations were held constant at 0.34 M and 0.0069 M respectively. The k_{obsd} values were determined by the slope of the plots of $\ln([LA]_0/[LA]_t)$ vs time. [b] Linear portion of plot which occurs after 5 h.

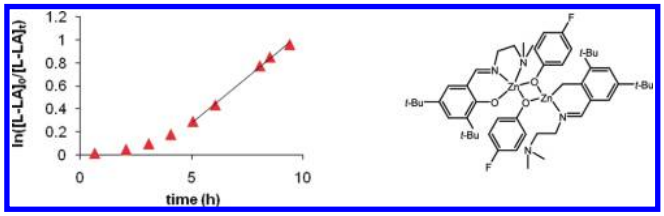

Figure 4. $\ln([LA]_0/[LA]_t)$ vs time plot for the ROP of L-lactide by the dimeric complex **6e** at ambient temperature.

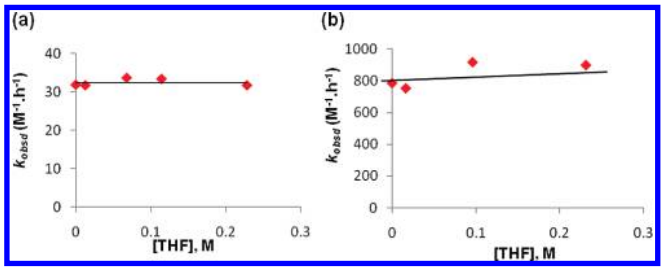

Figure 5. Independence of the rate constant for the ROP of L-lactide on the THF concentration in C_6D_6 at ambient temperature. (a) Complex **6a** as catalyst, (b) complex **6d** as catalyst.

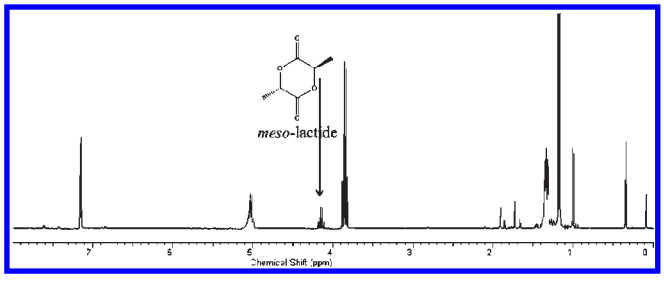

Figure 6. ^{1}H NMR spectrum in C_6D_6 during the ROP of L-lactide in the presence of complex **6d** at ambient temperature. Methine proton of *meso*-lactide observed at 4.15 ppm.

The resulting polylactides were isolated and purified by precipitation from CH_2Cl_2 with 5% HCl in methanol followed by drying in vacuo. The molecular weights and polydispersity indices of the purified polymers were determined by gel permeation chromatography (dual RI and light scattering detectors) in THF using polystyrene as a standard. These experimental findings indicate that the polymerization process is well-controlled (Table 3). The living character of the process can be noted by the low polydispersites over the range of 1.05−1.07, and the linear relationship between M_n and the monomer/initiator ratio as depicted in Figure 8.

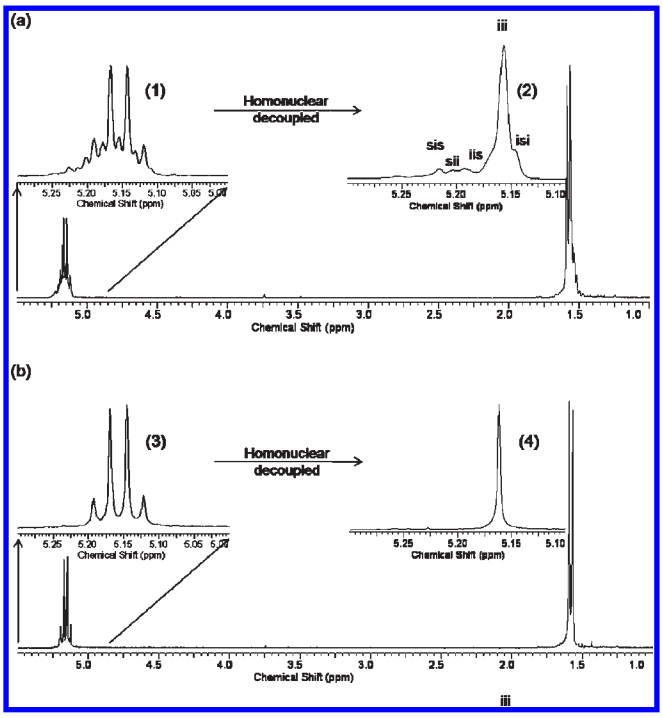

Figure 7. ^{1}H NMR spectra of polylactide in $CDCl_3$ prepared from L-lactide. (a) In the presence of complex **6d**, with **1**→**2** illustrating expanded methine region before and after homonuclear decoupling. (b) In the presence of complex **6a**, with **3**→**4** illustrating expanded methine region before and after homonuclear decoupling.

Table 3. Polylactides Produced from the ROP of *rac*-lactide in Chloroform at Ambient Temperature

				M_n			
entry	complex	M/I	conversion (%)[a]	theoretical[b]	GPC	$0.58M_{n,GPC}$[c]	PDI
1	**6a**	50	97	6 990	8 630	5 000	1.08
2	**6a**	300	96	41 509	96 191	55 790	1.05
3	**6a**	700	96	96 855	181 730	105 400	1.08
4	**6a**	1000	96	138 782	285 108	165 360	1.05
5	**6a**	2000	96	279 612	530 141	307 480	1.07
6	**6b**	50	98	7 062	8 161	4 730	1.31
7	**6c**	50	95	6 846	8 757	5 080	1.31
8	**6d**	50	98	7 062	8 171	4 740	1.13
9	**6e**	50	97	6 990	8 056	4 672	1.07

[a] Obtained from ^{1}H NMR spectroscopy. For entries 1 and 6 the reaction times were 2 h, all other reactions were carried out for 24 h. [b] Theoretical M_n = (M/I) × (% conversion) × (mol. wt. of lactide). [c] M_n values corrected by the equation: $M_n = 0.58M_{n,GPC}$.[114]

As previously mentioned the physical and degradation properties of polylactides are intimately dependent on the tacticity of the polymer. Herein we have examined the tacticity of the polymers resulting from the ROP of *rac*-lactide as catalyzed by the series of zinc derivatives, since

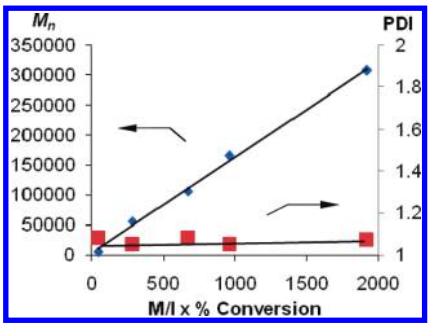

Figure 8. Linear relationship observed between M_n and monomer/initiator ratio of polylactide produced from *rac*-lactide catalyzed by complex **6a** at ambient temperature in $CHCl_3$.

the ligand's architecture is expected to play a major role in stereoselectivity.[18,115,116] Complexes **6a**−**d** were evaluated for the ROP of *rac*-lactide in $CHCl_3$ at various temperatures, and the afforded polymers' tacticities were assigned using the methine proton regions with homonuclear decoupling as described by Hillmyer and co-workers.[117]

P_r values were calculated from the ratio of the (area of isi and sis)/(total area in methine proton region) from the decoupled ^{1}H NMR spectra shown in Figure 9. As illustrated in Figures 9 and Table 4, complex **6c** produced the highest degree of heterotacticity in the polylactide produced from *rac*-lactide with a P_r = 0.83 at ambient temperature which increases to 0.89 at −30 °C. By way of contrast, the least sterically hindered zinc derivative, complex **6d**, provided polylactide with the lowest degree of heterotacticity (P_r = 0.68 at ambient temperature). In this latter instance, decreasing the polymerization temperature to −30 °C provided a P_r value of 0.87. Since the chiral center in complexes **6a**−**c** did not exhibit any selectivity in the ROP of L- or D-lactide, we suggest that the stereoselectivity in the polymerization of *rac*-lactide occurs via a chain-end mechanism.[52] Because the steric bulk of the ligands in complexes **6a** and **6b** is rather remote relative to the metal center, this rate effect may be due to a more facile dissociation of the dimethylamine arm during the polymerization process involving these catalysts. Indeed, Mehrkhodavandi and co-workers have shown in related diamino-phenol zinc complexes that the dimethylamine arm of the ligand is hemilabile.[101] To examine this possibility, we carried out an experiment where 6 equiv of 2-methylcyclohexanone were added to complex **6d** in C_6D_6. As seen in Figure 10, ^{1}H NMR spectroscopy reveals a significant portion of the complex showed the dimethylamine arm free with presumably concomitant binding of the ketone to the metal center via the oxygen donor. This binding would closely mimic the coordination of the lactide monomer to the zinc center. This reaction pathway would also account for the greatly reduced activity and highest heterotacticity exhibited by complex **6c** which contains the methylthio group. Nevertheless, inconsistent with an amine dissociation mechanism and lactide ROP reactivity is the observation that complex **6d** in the presence of excess THF exhibited a similar amine lability (Figure 11). However, as

(114) The M_n values for polylactide were corrected from the M_n values determined by GPC vs polystyrene standards, according to the equation $M_n = 0.58M_{n,GPC}$, as previously reported in the literature. (a) Barak, I.; Dubois, P.; Jérôme, R.; Teyssié, Ph *J. Polym. Sci., Part A: Polym. Chem.* **1993**, *31*, 305. (b) Baran, J.; Duda, A.; Kowalski, A.; Szymanski, R.; Penczek, S. *Macromol. Rapid Commun.* **1997**, *18*, 325–333.

(115) MacDonald, R. T.; McCarthy, S. P.; Gross, R. A. *Macromolecules* **1996**, *29*, 7356–7361.

(116) Stevels, W. M.; Ankone, M. J. K.; Dijkstra, P. J.; Feijen, J. *Macromolecules* **1996**, *29*, 6132–6138.

(117) Zell, M. T.; Padden, B. E.; Paterick, A. J.; Thakur, K. A. M.; Kean, R. T.; Hillmyer, M. A.; Munson, E. J. *Macromolecules* **2002**, *35*, 7700–7707.

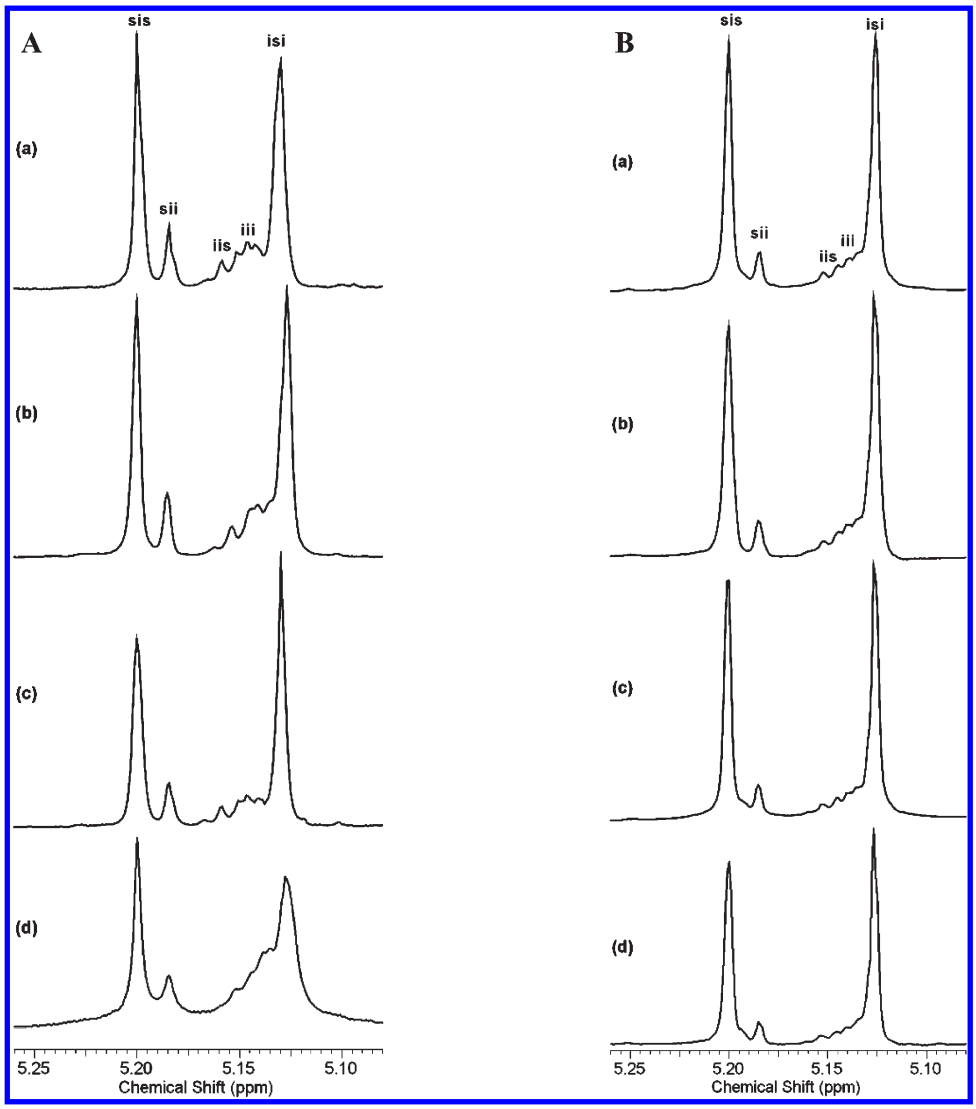

Figure 9. Homonuclear decoupled ^{1}H NMR ($CDCl_3$, 500 MH_3) spectra of the methine region of polylactide produced from *rac*-lactide with catalyst (a) **6a**, (b) **6b**, (c) **6c**, and (d) **6d**. (**A**) Polymerization temperature ambient. (**B**) Polymerization temperature −30 °C.

Table 4. P_r Values of Poly(*rac*-lactide) at Different Temperature[a,b]

complex	P_r at −30 °C	P_r at 0 °C	P_r at 22 °C
6a	88	81	76
6b	85	80	76
6c	89	86	83
6d	87	79	68

[a] Each reaction was performed in $CHCl_3$ at different temperatures. [b] P_r values were calculated from the ratio of the (area of isi and sis)/(total area in methine proton region).

noted in Figure 5 the addition of THF did not inhibit the ROP of L-lactide.

A point worthwhile noting regarding the measurement of P_r values from ^{1}H NMR peak areas is that the relative peak areas presented in Table 4 were measured multiple times with a planimeter.[118] In general, we have observed this method provides lower P_r values than those routinely determined by programs provided for deconvolutions by NMR software providers. For example, complex **6c** gave a P_r value of 0.89 at −30 °C for the polylactide produced from *rac*-lactide, whereas the FIT deconvolution program provided by Varian Instruments yielded a value of 0.98. Hence, we conclude that P_r values determined by this latter technique overestimate the heterotacticity of the thus formed polylactide.

The dependence of the thermal properties on the tacticity of the polylactides synthesized can be readily gleamed from the DSC measurements listed in Table 5. As is readily seen in Table 5, the isotactically pure polylactide afforded from the ROP of L-lactide by complex **6a** is highly crystalline and possesses a T_g value of 60 °C, with T_c and T_m values of 90 and 178 °C, respectively. On the other hand, the heterotactically enriched polymers provided by complexes **6a** and **6c** from the ROP of *rac*-lactide exhibited T_g parameters which increased with increasing P_r values. That is, complex **6a** which gave a polymer with

(118) From expanded versions of the ^{1}H NMR spectra illustrated in Figure 9, and assuming the sis and isi peaks are symmetrical, the areas of these peaks vs that of the total methine proton region were measured using a planimeter. This mechanical integrating instrument used to measure the area under a curve by moving a point attached to an arm of the device around the perimeter of the defined curve can be easily demonstrated to accurately assess areas as indicated by concomitant area measurements of known dimensions.

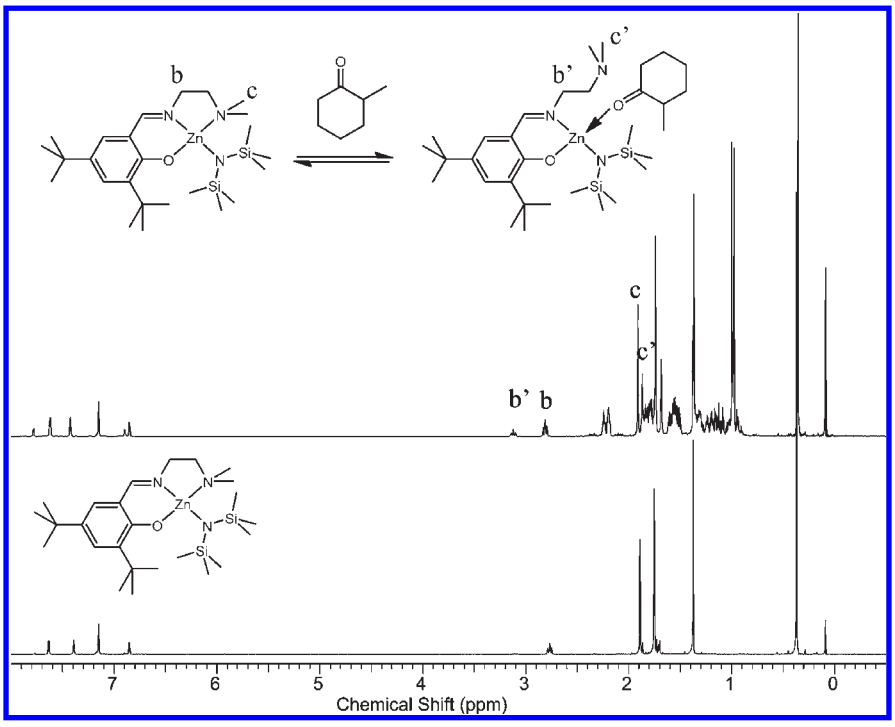

Figure 10. ^{1}H NMR spectrum (C_6D_6, rt) of **6d** before addition of 2-methylcyclohexanone (bottom) and 15 min after addition of 6 equiv of 2-methylcyclohexanone (top).

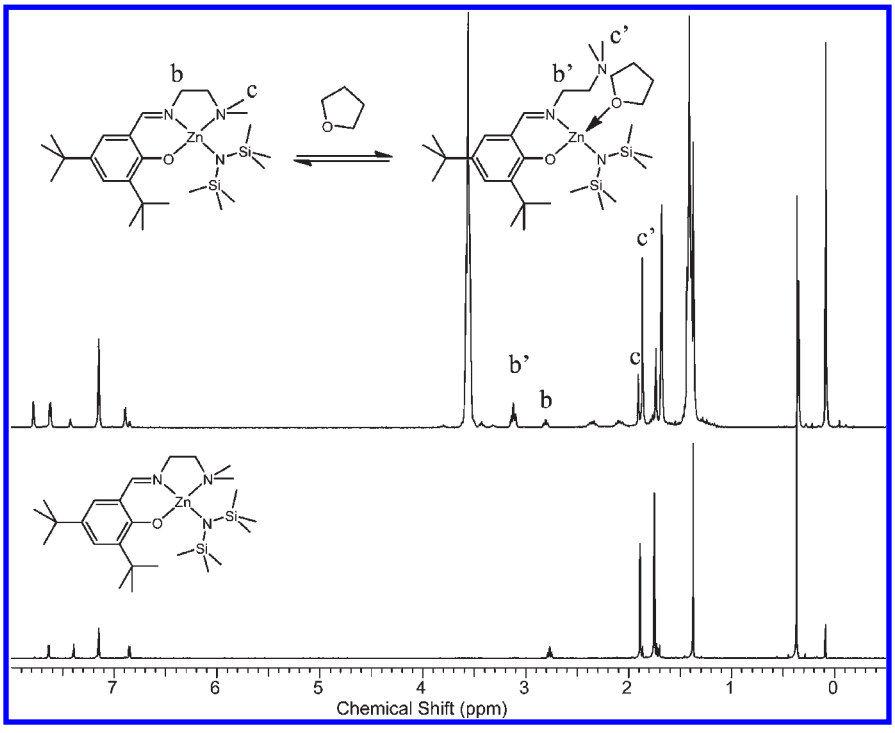

Figure 11. ^{1}H NMR spectrum (C_6D_6, rt) of **6d** before addition of THF (bottom) and 15 min after addition of 10 equiv of THF (top).

a P_r value of 0.76 has a T_g of 39 °C, and complex **6c** which provided a polymer with a P_r of 0.89 has a T_g of 50 °C.

Summary Remarks

Herein we have reported a new series of well-characterized chiral tridentate Schiff base ligands and their zinc complexes. The complexes are shown to be active toward the ROP of lactide. The polymerization processes appear to be living systems as depicted by a linear relationship between M_n and % conversion, as well as, a low polydispersity index. Experimental results revealed that enantiomeric pure complexes did not preferably polymerize one enantiomer over the other as is evident from the ratios of $k_{D(obsd)}/k_{L(obsd)}$ being close to 1 for all catalysts investigated. However, the substituent of the chiral tridentate Schiff base ligands played a major role in producing heterotactic polylactide from *rac*-lactide, and it

Table 5. Physical and Thermal Properties of Polylactides

complex	M/I	lactide	tacticity	M_n	decomposition temp. (°C)	T_g[a] (°C)	T_c[a] (°C)	T_m[a] (°C)
6a	50	L-lactide	isotactic	N/A[b]	300	60	90	178
6a	50	*rac*-lactide	hetero(P_r = 0.76)	8630	300	39		
6c	50	*rac*-lactide	hetero(P_r = 0.89)	8760	300	50		

[a] Determined from second heating run. [b] Molecular weight was not measured because of polymer's insolubility in THF due to its high crystallinity.

Table 6. Crystallographic Data for Complexes **6a**−**6d**

	6a	**6b**	**6c**	**6d**	**6e**
empirical formula	$C_{32}H_{55}N_3OSi_2Zn$	$C_{58}H_{114}N_6O_2Si_4Zn_2$	$C_{33}H_{67}N_3OSSi_2Zn$	$C_{55}H_{108}N_6O_2Si_4Zn_2$	$C_{50}H_{70}F_2N_4O_4Zn_2$
fw	619.34	1170.65	675.51	1128.57	959.84
temperature (K)	150(2) K	110(2) K	110(2) K	110(2) K	110(2) K
crystal system	orthorhombic	monoclinic	monoclinic	monoclinic	monoclinic
space group	*P*(2)1(2)1(2)1	*P*2(1)	*P*2(1)	*P*2(1)/*c*	*P*2(1)/*n*
a(Å)	8.719(4)	10.616(3)	15.315(7)	13.530(5)	12.128(12)
b(Å)	16.535(8)	18.225(4)	10.089(5)	23.298(5)	21.45(2)
c(Å)	24.901(12)	17.992(4)	26.190(13)	10.488(5)	20.25(2)
α(deg)	90	90	90	90.000(5)	90
β(deg)	90	91.995(13)	104.946(6)	99.190(5)	105.529(12)
γ(deg)	90	90	90	90.000(5)	90
V(Å)	3590(3)	3478.7(14)	3910(3)	3264(2)	5074(9)
D_c(Mg/m^3)	1.146	1.118	1.148	1.148	1.257
Z	4	2	4	2	4
abs coeff (mm^{-1})	0.777	1.805	0.770	0.848	0.997
reflections collected	32055	27837	44430	22528	48125
independent reflections	7063 [*R*(int) = 0.1231]	9520 [*R*(int) = 0.0627]	17705 [*R*(int) = 0.0242]	4681 [*R*(int) = 0.1202]	11309 [*R*(int) = 0.0242]
data/restrains/parameters	7063/4/373	9520/4/694	17705/44/818	4681/2/337	11309/0/575
GOF on F^2	1.014	1.077	1.032	0.965	1.036
final *R* indices	R_1 = 0.0539	R_1 = 0.0402	R_1 = 0.0347	R_1 = 0.0756	R_1 = 0.0932
[$I > 2\sigma$(I)]	R_w = 0.1190	R_w = 0.0963	R_w = 0.0899	R_w = 0.1935	R_w = 0.2505
final *R* indices	R_1 = 0.0779	R_1 = 0.0515	R_1 = 0.0408	R_1 = 0.1165	R_1 = 0.1435
(all data)	R_w = 0.1299	R_w = 0.1030	R_w = 0.0927	R_w = 0.2405	R_w = 0.3180

was shown that complex **6c** produced the highest degree of heterotactic polylactide with P_r values of 0.83 and 0.89 at ambient and −30 °C, respectively. As might be anticipated, the T_g of the heterotactic polylactides increased significantly as the degree of heterotacticity increased.

Experimental Section

Methods and Materials. All manipulations were carried out using a double manifold Schlenk vacuum line under an argon atmosphere or an argon filled glovebox unless otherwise stated. Toluene and THF were freshly distilled from sodium/benzophenone before use. Methanol and dichloromethane were purified by an MBraun Manual Solvent Purification System packed with Alcoa F200 activated alumina desiccant. Pentane was freshly distilled from CaH_2. Deuterated chloroform and deuterated benzene from Cambridge Isotope Laboratories Inc. were stored in the glovebox and used as received. L- and D-lactide were gifts from PURAC America Inc., and *rac*-lactide was purchased from Aldrich. These lactides were recrystallized from toluene, dried under vacuum at 40 °C overnight, and stored in the glovebox. Sodium *bis*(trimethylsilyl)amide and *p*-fluophenol were purchased from Alfa Aesar, zinc chloride anhydrous was purchased from Strem Chemicals, and all were stored in the glovebox. *N*-Boc-L-phenylalanine, *N*-Boc-L-methionine, and *N*-Boc-L-leucine were purchased from Chem-Impex international and used as received. *N,N*-dimethylethylendiamine was purchased from Acros and used as received. 3,5-Di-*tert*-butyl-2-hydroxybenzaldehyde and zinc(bis-trimethylsilyl amide)$_2$ were prepared according to published procedure.[75,76,119,120] All other compounds and reagents were obtained from Aldrich and were used without further purification. Analytical elemental analysis was provided by Canadian Microanalytical Services Ltd.

Measurements. ^{1}H NMR spectra were recorded on Unity+ 300 MHz and VXR 300 MHz superconducting NMR spectrometers. Molecular weight determinations were carried out with Viscotek Modular GPC apparatus equipped with ViscoGEL I-series columns (H + L) and Model 270 dual detector composed of refractive index and light scattering detectors. TGA measurements were performed with TGA 1000 Thermogravimetric Analyzer by Instrument Specialists Incorporated. The samples were scanned from room temperature to the desired temperature under argon atmosphere with a heating rate of 5 °C/min. DSC measurements were performed with a Polymer DSC by Mettler Toledo. The samples were scanned from −100 to 200 °C under nitrogen atmosphere. The glass transition temperature (T_g), the crystallization temperature (T_c), and the melting temperature (T_m) of polylactides were determined from the second heating at a heating rate of 5 °C/min. X-ray crystallography was done on a Bruker Smart 1000 diffractometer equipped with a CCD detector in a nitrogen cold stream maintained at 110 K. Crystal data and details of the data collection for complexes **6a**−**6e** are provided in Table 6.

General Procedure for Synthesis of Chiral Diamines 4a−**c.** The chiral diamines **4a**−**c** were prepared according to the reported literature[111] with some modifications. To *N*-Boc-L-phenylalanine (75 mmol) in CH_2Cl_2 (200 mL) was added DCC (83 mmol) followed by HOBt (83 mmol) at ambient temperature. The dimethylamine (83 mmol, 40% aq solution) was added after 2 h. The reaction mixture was stirred overnight, and the solvent was removed under reduced pressure to obtain a white precipitate. The white precipitate was removed by filtration, and the filtrate was washed with 10% citric acid solution followed by washing with a saturated $NaHCO_3$ solution. The organic layer was separated, dried over $NaSO_4$, and concentrated to dryness under reduced pressure to afford the crude amides **2a**−**c** which were used in the next step without further purification.

(119) Darensbourg, D. J.; Holtcamp, M. W.; Struck, G. E.; Zimmer, M. S.; Niezgoda, S. A.; Rainey, P.; Robertson, J. B.; Draper, J. D.; Reibenspies, J. H. *J. Am. Chem. Soc.* **1999**, *121*, 107–116.
(120) Hansen, T. V.; Skattebøl, L. *Tetrahedron Lett.* **2005**, *46*, 3829–3830.

The *N*-Boc-protected amines were then deprotected with TFA. To a solution of *N*-Boc-protected amines **2a**−**c** (55 mmol) in anhydrous CH_2Cl_2 (15 mL), TFA (165 mmol) was added and stirred for overnight at room temperature. Excess TFA and solvent were removed under reduced pressure. The resulting yellowish oil was neutralized with sat. $NaHCO_3$, extracted with CH_2Cl_2 (10 × 30 mL), dried over Na_2SO_4, and evaporated to dryness. The crude amides **3a**−**c** were used for the next step without purification.

The amides **3a**−**c** (45 mmol) were dissolved in THF (30 mL) and cannulated into a suspension of $LiAlH_4$ (180 mmol) in THF (60 mL) cooled in an ice bath. The reaction mixture was heated to reflux overnight. The mixture was placed in an ice bath, and EtOAc (100 mL) was slowly added to the mixture, followed by saturated Na_2SO_4 (100 mL). The resulting white solid was washed with EtOAc (3× 50 mL). The combined organic layers were dried over Na_2SO_4, and the solvent was removed under reduced pressure to afford slightly yellow oils **4a**−**c**. The crude products **4a**−**c** were purified by vacuum distillation in a short-path apparatus.

(*S*)-*N*′,*N*′-dimethyl-3-phenylpropane-1,2-diamine 4a. Following the general procedure for synthesis of chiral diamines, the title compound **4a** was purified by vacuum distillation (0.5−0.7 mmHg) in a short-path apparatus at 121 °C; 4.36 g of yellowish liquid was collected (61% yield). $[\alpha]_D = +12.64$ ($c = 1.1$, $CHCl_3$); ^{1}H NMR (300 MHz, $CDCl_3$) δ = 1.20−1.80 (br s, 2H), 2.13−2.19 (m, 1H), 2.23 (s, 6H), 2.27−2.31 (m, 1H), 2.47 (dd, J = 13.46, 8.8 Hz, 1H), 2.74 (dd, J = 13.25, 4.5 Hz, 1H), 3.09−3.18 (m, 1H), 7.19−7.25 (m, 3H), 7.26−7.32 (m, 2H); ^{13}C NMR (300 MHz, $CDCl_3$) δ = 49.25, 52.05, 53.35, 68.46, 116.28, 118.08, 118.78, 126.78. Anal. Calcd for $C_{11}H_{18}N_2$: C, 74.11; H, 10.18; N, 15.71. Found: C, 71.98; H, 10.26; N, 14.56. HRMS (ESI), m/z, 179.1591 [M+H$^+$], calcd for $C_{11}H_{18}N_2$, 179.15.

(*S*)-*N*′,*N*′,4-trimethylpentane-1,2-diamine 4b. Following the general procedure for synthesis of chiral diamines, the title compound **4b** was purified by vacuum distillation (0.5−0.7 mmHg) in a short-path apparatus at 110 °C; 3.75 g of product was collected (59% yield). $[\alpha]_D^{20} = +27.77$ (c = 1.8, $CHCl_3$); ^{1}H NMR (300 MHz, $CDCl_3$) δ = 0.89 (d, J = 7.0 Hz, 3H), 0.91 (d, J = 6.9 Hz, 3H), 1.11−1.24 (m, 2H), 1.69−1.80 (m, 1H), 2.06 (dd, J = 12.0, 3.8 Hz, 1H), 2.12−2.19 (m, 1H), 2.15 (br s, 2H), 2.22 (s, 6H), 2.90−2.98 (m, 1H); ^{13}C NMR (300 MHz, $CDCl_3$) δ = 22.00, 23.52, 24.60, 45.09, 45.81, 45.99, 67.43. Anal. Calcd for $C_8H_{20}N_2$: C, 66.61; H, 13.97; N, 19.42. Found: C, 61.97; H, 13.34; N, 16.53. HRMS (ESI), m/z, 144.1523 [M+H$^+$], calcd for $C_8H_{20}N_2$, 144.15.

(*S*)-*N*′,*N*′-dimethyl-4-(methylthio)butane-1,2-diamine 4c. Following the general procedure for synthesis of chiral diamines, the title compound **4c** was purified by vacuum distillation (1.2 mmHg) in a short-path apparatus at 125 °C; 4.22 g of product was collected (40% yield). $[\alpha]_D^{21} = +12.22$ (c = 1.14, $CHCl_3$); ^{1}H NMR (300 MHz, $CDCl_3$) δ = 1.29−1.43 (m, 2H), 1.76−1.86 (m, 2H), 1.88 (s, 3H), 2.00 (s, 6H), 2.30−2.46 (m, 2H), 2.71−2.81 (m, 2H); ^{13}C NMR (300 MHz, $CDCl_3$) δ = 15.39, 30.74, 35.04, 45.49, 47.33, 66.68. Anal. Calcd for $C_7H_{18}N_2S$: C, 51,80; H, 11.18; N, 17.26; S, 19.76 Found: C, 51.51; H, 10.97; N, 15.11; S, 17.09. HRMS (ESI), m/z, 163.1309 [M+H$^+$], calcd for $C_7H_{18}N_2S$, 163.13.

General Procedure for Synthesis of Tridentate Schiff Base Ligands. 3,5-Di-*tert*-butyl-2-hydroxybenzaldehyde[75,76,120] (1.0 equiv) in MeOH (30 mL) was added to **4a**−**d**, (1.0 equiv). The solution mixture was heated to reflux overnight and dried over Na_2SO_4 followed by filtration. The volatile component was removed in vacuo to obtain tridentate Schiff base ligands **5a**−**d** in 88% to quantitative yield.

(*S*,*E*)-2,4-di-*tert*-butyl-6-((1-(dimethylamino)-3-phenylpropan-2-ylimino)methyl)phenol (L^1-H) 5a. Following the general procedure for synthesis of tridentate Schiff base ligands, 3,5-di-*tert*-butyl-2-hydroxybenzaldehyde (1.26 g, 5.38 mmol) in MeOH (30 mL) was added to **4a** (0.958 g, 5.38 mmol). The solution mixture was heated to reflux overnight and dried over Na_2SO_4 followed by filtration. The volatile component was removed in vacuo to obtain **5a** in 95% yield. $[\alpha]_D^{20} = -154.54$ (c = 1.1, $CHCl_3$); ^{1}H NMR (300 MHz, $CDCl_3$) δ = 1.37 (s, 9H, C(CH_3)$_3$), 1.55 (s, 9H), 2.35 (s, 6H), 2.55−2.68 (m, 2H), 2.95 (dd, J = 13.39, 8.33 Hz, 1H), 3.13 (dd, J = 13.39, 4.16 Hz, 1H), 3.54−3.63 (m, 1H), 7.03 (d, 7.03 (d, J = 2.87 Hz, 1H), 7.23−7.32 (m, 5H, PhH), 7.44 (d, J = 2.65 Hz,1H), 8.13 (s, 1H), 13.89 (s, 1H, OH); ^{13}C NMR (300 MHz, $CDCl_3$) δ = 29.58, 31.62, 34.21, 35.13, 41.14, 46.34, 65.14, 69.86, 117.90, 126.10, 126.28, 126.83, 128.41, 129.74, 136.54, 138.89, 139.83, 158.25, 165.63. Anal. Calcd for $C_{26}H_{38}N_2O$: C, 79.14; H, 9.71; N, 7.10. Found: C, 78.56; H, 9.69; N, 6.93. HRMS (ESI), m/z, 395.3184 [M+H$^+$], calcd for $C_{26}H_{38}N_2O$, 395.31.

(*S*,*E*)-2,4-di-*tert*-butyl-6-((1-(dimethylamino)-4-methylpentan-2-ylimino)methyl)phenol (L^2-H) 5b. Following the general procedure for synthesis of tridentate Schiff base ligands, 3,5-di-*tert*-butyl-2-hydroxybenzaldehyde (1.30 g, 5.54 mmol) in MeOH (30 mL) was added to **4a** (0.799 g, 5.54 mmol). The solution mixture was heated to reflux overnight and dried over Na_2SO_4 followed by filtration. The volatile component was removed in vacuo to obtain **5b** in 96% yield. $[\alpha]_D^{21} = -18.72$ (c = 1.17, $CHCl_3$); ^{1}H NMR (300 MHz, $CDCl_3$) δ = 0.87 (dd, J = 10.37, 5.88 Hz, 6H), 1.32 (s, 9H), 1.46 (s, 9H), 1.43−1.46 (m, 1H), 1.55−1.65 (m, 1H), 2.25 (s, 6H), 2.42−2.46 (m, 2H), 3.34−3.43 (m, 1H), 7.11 (d, J = 2.60 Hz, 1H), 7.38 (d, J = 2.60 Hz, 1H), 8.34 (s, 1H), 13.89 (s, 1H, OH); ^{13}C NMR δ = (300 MHz, $CDCl_3$) δ = 21.46, 23.89, 24.44, 29.59, 33.66, 34.26, 35.13, 43.36, 46.40, 65.14, 117.96, 126.06, 126.79, 136.65, 139.90, 158.37, 165.02. Anal. Calcd for $C_{23}H_{40}N_2O$: C, 76.61; H, 11.18; N, 7.77. Found: C, 76.19; H, 11.05; N, 7.36. HRMS (ESI), m/z, 361.3292 [M+H$^+$], calcd for $C_{23}H_{40}N_2O$, 361.31.

(*S*,*E*)-2,4-di-*tert*-butyl-6-((1-(dimethylamino)-4-(methylthio)-butan-2-ylimino)methyl)phenol (L^3-H) 5c. Following the general procedure for synthesis of tridentate Schiff base ligands, 3,5-di-*tert*-butyl-2-hydroxybenzaldehyde (1.03 g, 4.41 mmol) in MeOH (30 mL) was added to **4a** (0.72 g, 4.41 mmol). The solution mixture was heated to reflux overnight and dried over Na_2SO_4 followed by filtration. The volatile component was removed in vacuo to obtain **5c** in 88% yield. $[\alpha]_D^{21} = -62.80$ (c = 1.21, $CHCl_3$); ^{1}H NMR (300 MHz, $CDCl_3$) δ = 1.33 (s, 9H), 1.46 (s, 9H), 1.84−2.08 (m, 2H), 2.10 (s, 3H), 2.26 (s, 6H), 2.38−2.65 (m, 4H), 3.44−3.56 (m, 1H), 7.12 (d, J = 2.63 Hz, 1H), 7.39 (d, J = 2.63 Hz, 1H), 8.39(s, 1H), 13.70 (s, 1H, OH); ^{13}C NMR (300 MHz, $CDCl_3$) δ = 15.57, 29.73, 31.11, 33.27, 34.26, 35.24, 46.45, 65.54, 66.52, 177.87, 126.32, 127.11, 136.75, 140.10, 158.39, 166.26. Anal. Calcd for $C_{22}H_{38}N_2OS$: C, 69.79; H, 10.12; N, 7.40; S, 8.47 Found: C, 69.88; H, 10.16; N, 7.17; S, 8.27. HRMS (ESI), m/z, 379.2673 [M+H$^+$], calcd for $C_{22}H_{38}N_2OS$, 379.27.

(*E*)-2,4-di-*tert*-butyl-6-((2-(dimethylamino)ethylimino)methyl)-phenol (L^4-H) 5d[121]. Following the general procedure for synthesis of tridentate Schiff base ligands, 3,5-di-*tert*-butyl-2-hydroxybenzaldehyde (2.00 g, 8.53 mmol) in MeOH (30 mL) was added to 4d (*N*′,*N*′-dimethylethane-1,2-diamine) (0.75 g, 8.53 mmol). The solution mixture was heated to reflux overnight and dried over Na_2SO_4 followed by filtration. The volatile component was removed in vacuo to obtain **5d** in 92% yield. ^{1}H NMR (300 MHz, $CDCl_3$) δ = 1.32 (s, 9H), 1.65 (s, 9H), 2.02 (s, 6H), 2.28 (t, J = 7.03, 2H), 3.31 (t, J = 7.03, 2H), 6.98 (d, J = 2.52, 1H), 7.56 (d, J = 2.52, 1H), 7.84 (s, 1H), 14.26 (s, 1H, OH); ^{13}C NMR (300 MHz, $CDCl_3$) δ = 29.8, 31.7, 34.3, 35.4, 45.7, 57.8, 60.1, 118.7, 126.3, 126.7, 137.1, 140.0, 158.9, 166.8. Anal. Calcd for $C_{19}H_{32}N_2O$: C, 74.95; H, 10.59; N, 9.20. Found: C, 74.94; H, 10.61; N, 9.02. HRMS (ESI), m/z, 305.2620 [M+H$^+$], calcd for $C_{19}H_{32}N_2O$, 305.25.

(121) Cameron, P. A.; Gibson, V. C.; Redshaw, C.; Segal, J. A.; Bruce, M. D.; White, A. J. P.; Williams, D. J. *Chem. Commun.* **1999**, 1883–1884.

General Procedure for Synthesis of Tridentate Schiff Base Zinc Complexes (L^{1-4}-H) 6a−d. A Tridentate Schiff base ligand (1 equiv) was dissolved in pentane and was cannulated to a solution of $Zn[N(SiMe_3)_2]_2$ (1.0 equiv) in pentane. The reaction mixture was stirred until a yellow precipitate was formed and allowed to stir at room temperature for an additional 3 h. The resulting yellow precipitate was then washed with cold pentane (3× 2 mL). The volatile component was removed under reduced pressure to obtain light yellow solid **6a−d**.

Synthesis of [L^1ZnN(SiMe$_3$)$_2$] 6a. A Tridentate Schiff base ligand **5a** (1.06 g, 2.68 mmol) was dissolved in pentane (3 mL) and was cannulated to a solution of $Zn[N(SiMe_3)_2]_2$ (1.04 g, 2.68 mmol) in pentane (1 mL). The reaction mixture was stirred until a yellow precipitate was formed and allowed to stir at room temperature for an additional 3 h. The resulting yellow precipitate was then washed with cold pentane (3× 2 mL). The volatile component was removed under reduced pressure to obtain light yellow solid **6a** in 51% yield. $[\alpha]_D^{21} = +67.50$ (c = 1.02, C_6D_6); ^{1}H NMR (300 MHz, C_6D_6) δ = 0.43 (s, 18H), 1.36 (s, 9H), 1.57−1.66 (m, 1H), 1.76 (s, 9H), 1.82 (s, 6H), 2.35−2.47 (m, 2H), 2.67−2.74 (m, 1H), 3.14−3.24 (m, 1H), 6.75 (d, J = 2.95 Hz, 1H), 6.93 (d, 1H), 6.96 (d, 1H), 7.09−7.18 (m, 3H), 7.45 (s, 1H), 7.63 (d, J = 2.53, 1H); ^{13}C NMR (300 MHz, C_6D_6) δ = 6.20, 30.04, 31.69, 34.02, 36.11, 39.91, 45.41, 61.89, 63.28, 118.24, 127.25, 128.33, 129.09, 129.63, 129.85, 137.17, 142.05, 168.56, 170.82, 165.63; Anal. Calcd for $C_{32}H_{55}N_3OSi_2Zn$: C, 62.05; H, 8.95; N, 6.78. Found: C, 62.48; H, 8.55; N, 6.07.

Synthesis of [L^2ZnN(SiMe$_3$)$_2$] 6b. A Tridentate Schiff base ligand **5b** (1.08 g, 2.97 mmol) was dissolved in pentane (3 mL) and was cannulated to a solution of $Zn[N(SiMe_3)_2]_2$ (1.15 g, 2.97 mmol) in pentane (1 mL). The reaction mixture was stirred until a yellow precipitate was formed and allowed to stir at room temperature for an additional 3 h. The resulting yellow precipitate was then washed with cold pentane (3× 2 mL). The volatile component was removed under reduced pressure to obtain light yellow solid **6b** in 50% yield. $[\alpha]_D^{21} = +89.82$ (c = 1.00, C_6D_6); ^{1}H NMR (300 MHz, $CDCl_3$) δ = 0.4 (s, 18H), 0.72 (dd, J = 11.25, 5.62 Hz, 6H), 1.38 (s, 9H), 1.78 (s, 9H), 1.82 (bs, 2H), 1.94 (s, 6H), 2.16 (m, 2H), 2.42 (bs, 1H), 3.13−3.27 (m, 1H), 7.03 (d, J = 3.03 Hz, 1H), 7.66 (d, J = 3.03 Hz, 1H), 7.86 (s, 1H); ^{13}C NMR (300 MHz,C_6D_6) δ = 2.78, 6.19, 22.20, 23.26, 24.54, 30.09, 31.80, 34.15, 36.28, 41.83, 46.10, 58.26, 64.88, 118.66, 129.97, 135.09, 142.35, 168.59; Anal. Calcd for $C_{29}H_{57}N_3OSi_2Zn$: C, 59.50; H, 9.81; N, 7.18. Found: C, 59.63; H, 9.63; N, 6.66.

Synthesis of [L^3ZnN(SiMe$_3$)$_2$] 6c. A Tridentate Schiff base ligand **5c** (1.03 g, 2.73 mmol) was dissolved in pentane (3 mL) and was cannulated to a solution of $Zn[N(SiMe_3)_2]_2$ (1.05 g, 2.73 mmol) in pentane (1 mL). The reaction mixture was stirred until a yellow precipitate was formed and allowed to stir at room temperature for an additional 3 h. The resulting yellow precipitate was then washed with cold pentane (3× 2 mL). The volatile component was removed under reduced pressure to obtain light yellow solid **6c** in 55% yield. $[\alpha]_D^{21} = +115.70$ (c = 1.21, C_6D_6); ^{1}H NMR (300 MHz, $CDCl_3$) δ = 0.39 (s, 18H), 1.36 (s, 9H), 1.40−1.51 (m, 2H), 1.70 (s, 3H), 1.75 (s, 9H), 1.90 (s, 6H), 2.04−2.27 (m, 4H), 3.11−3.24 (m, 1H), 6.98 (d, J = 2.73 Hz, 1H), 7.64 (d, J = 2.73 Hz, 1H), 7.87 (s, 1H) ^{13}C NMR (300 MHz, $CDCl_3$) δ = 6.14, 15.23, 30.06, 30.26, 31.78, 32.50, 34.11, 36.18, 45.78, 59.33, 63.64, 118.46, 128.49, 129.99, 135.10, 142.14, 168.65, 170.03; Anal. Calcd for $C_{28}H_{55}N_3OSSi_2Zn$: C, 55.73; H, 9.91; N, 6.69; S, 5.31. Found: C, 55.68; H, 8.89; N, 6.05; S, 5.28.

Synthesis of [L^4ZnN(SiMe$_3$)$_2$] 6d. A Tridentate Schiff base ligand **5d** (1.00 g, 3.28 mmol) was dissolved in pentane (3 mL) and was cannulated to a solution of $Zn[N(SiMe_3)_2]_2$ (1.27 g, 3.28 mmol) in pentane. The reaction mixture was stirred until a yellow precipitate was formed and allowed to stir at room temperature for an additional 3 h. The resulting yellow precipitate was then washed with cold pentane (3× 2 mL). The volatile component was removed under reduced pressure to obtain light yellow solid **6d** in 52% yield. $[\alpha]_D^{21} = 0.00$ (c = 1.05, C_6D_6); ^{1}H NMR (300 MHz, $CDCl_3$) δ = 0.37 (s, 18H), 1.38 (s, 9H), 1.75 (s, 9H), 1.90 (s, 6H), 2.78 (t, J = 6.01 Hz, 2H), 3.11 (t, J = 6.01 Hz, 2H), 6.85 (d, J = 2.7 Hz, 1H), 7.40 (s, 1H), 7.63 (d, J = 2.7 Hz, 1H); ^{13}C NMR (300 MHz, $CDCl_3$) δ = 6.10, 30.06, 31.84, 34.06, 36.29, 45.64, 52.99, 57.22, 59.67, 60.33, 118.66, 129.79, 135.14, 142.26, 169.87. Anal. Calcd for $C_{25}H_{49}N_3OSi_2Zn$: C, 56.73; H, 9.33; N, 7.94. Found: C, 57.91; H, 8.61; N, 7.18.

Synthesis of [L^1ZnOPh] 6e. A Tridentate Schiff base ligand **5a** (0.55 g, 1.82 mmol) and *p*-fluorophenol (0.24 g, 1.82 mmol) were dissolved in pentane (3 mL) and was cannulated to a solution of $Zn[N(SiMe_3)_2]_2$ (0.74 g, 1.82 mmol) in pentane (1 mL). The reaction mixture was stirred until a yellow precipitate was formed and allowed to stir at room temperature for an additional 3 h. The resulting yellow precipitate was then washed with cold pentane (3× 2 mL). The volatile component was removed under reduced pressure to obtain light yellow solid **6e** in 55% yield. ^{1}H NMR (300 MHz, $CDCl_3$) δ = 1.39 (s, 9H), 1.76 (s, 9H), 1.99 (s, 6H), 2.80 (t, J = 5.72 Hz, 2H), 3.11 (t, J = 5.72 Hz, 2H), 6.70 (t, J = 8.78 Hz, 2H), 6.91 (bs, 2H), 7.02 (d, J = 2.72 Hz, 1H), 7.77 (m, 2H); ^{13}C NMR (300 MHz, $CDCl_3$) δ = 30.10, 30.36, 31.77, 34.12, 36.05, 45.50, 46.31, 54.44, 57.17, 59.57, 115.75, 116.04, 118.10, 119.50, 129.82, 135.49, 141.75, 169.67, 171.81, Anal. Calcd for $C_{25}H_{35}FN_2O_2Zn$: C, 62.56; H, 7.35; N, 5.84; F, 3.96. Found: C, 62.83; H, 7.54; N, 5.89; F, 3.84.

Polymerization Procedure. In a typical experiment (Table 3, entry 1), in the glovebox, a Schlenk flask was charged with a solution of complex **6a** (8.58 mg, 13.87 μmol) in $CHCl_3$ (2 mL). To this solution was added *rac*-lactide (100 mg, 0.69 mmol, 50 equiv). The mixture was stirred at room temperature for 60 min. After a small sample of the crude solution was removed with a syringe to be characterized by ^{1}H NMR spectroscopy, the product was isolated and purified by precipitation from dichloromethane by the addition of 5% hydrochloric acid in methanol. The polymer was collected and dried under vacuum to constant weight.

Kinetic Studies. Polymerizations of L- or D-lactide using complexes **6a−d** were monitored by ^{1}H NMR spectroscopy. Each monomer and corresponding zinc complex were dissolved in C_6D_6, and the % conversion was investigated from the integration of polymer and monomer signals. The chemical shifts of polylactide are 5.01 (q, H) and 1.32 (d, CH_3), and the chemical shifts of lactide monomer are 3.79 (q, H) and 1.16 (d, CH_3).

Acknowledgment. We gratefully acknowledge the financial support of the National Science Foundation (CHE-05-43133) and the Robert A. Welch Foundation (A-0923). We also thank PURAC America, Inc. for providing lactide samples for this research. Stephanie Wilson is also acknowledged for some of the preliminary studies she carried out on ligand synthesis during an NSF REU program.

Supporting Information Available: X-ray crystallographic files in CIF format for the structural determinations of complexes **6a−e**. This material is available free of charge via the Internet at http://pubs.acs.org.